Isoplanatism, and high spatial resolution solar imaging

Abdanour Irbah, Julien Borgnino, Francis Laclare, Guy Merlin

Astron. Astrophys. 276, 663–672 (1993)

ASTRONOMY AND ASTROPHYSICS

Isoplanatism and high spatial resolution solar imaging

A. Irbah[1], J. Borgnino[2], F. Laclare[3], and G. Merlin[3]

[1] Observatoire d'ALGER, CRAAG, B.P. 63 Bouzareah, Alger, Algerie
[2] Départment d'Astrophysique-Université de Nice-Sophia Antipolis, Faculté des Sciences, F-06108 Nice Cedex 2, France
[3] Observatoire de la Côte d'Azur, CERGA, Avenue Copernic, F-06130 Grasse, France

Received July 2, 1992; accepted February 22, 1993

Abstract. A method is presented allowing one to estimate, in the case of daytime observations, the angle-of-arrival isoplanatic patch size from the measurement of the differential image motion of the solar limb. The experimental results have been obtained using the solar astrolabe of Calern Observatory (CERGA-France). Performing a modelization as proposed by Fried (1977) leads to an explanation of these results by an equivalent atmosphere formed with two impulse turbulent layers corresponding to two different scales for the size of the isoplanatic patch. Finally, the isoplanatism is quantified for speckle interferometry and adaptive optics experiments.

Key words: atmospheric effects – methods: observational – techniques: image processing – Sun: general – Sun: photosphere

1. Introduction

The formation of astronomical images through the terrestrial atmosphere by means of ground-based telescopes is generally formalized as a convolution product which expresses a spatial-frequency linear filtering. By using this formalism, one assumes in particular that the point spread function of the whole system, telescope and atmosphere, is invariant over the observation field. If one considers wavefronts coming from a point source through the atmospheric turbulent layers, they appear randomly perturbed, in space and time, which gives consequently a random behaviour to this point spread function. At any moment, one can consider that the point spread function is invariant only on a precise patch, named the isoplanatic patch, of the observation field and that it follows well-determined characteristics of the perturbations due to the atmosphere.

The importance of knowledge of this patch size has increased with the development of high-angular-resolution observation techniques (real-time and post-detection image restoration) which allow one to overcome the optical effects due to atmospheric turbulence and to reach the theoretical resolution of the instruments. Thus, in adaptive optics, the creation of laser backscattered reference stars (Foy & Labeyrie 1985) which would lead to the measurement of the wavefront and then to real-time compensation of the atmospherical effects has to be elaborated by taking into account the constraints related to the size of the isoplanatic patch (Welsh et al. 1991; Séchaud et al. 1990; Chassat 1989). Similarly, for image reconstruction techniques applied to extended astronomical objects (Sun, multiple star systems, ...), it is necessary to break up the image into an array in which each element to be corrected has to be smaller than the isoplanatic patch size (Von Der Lühe 1988).

This paper has been conceived as a contribution to the study of the angle-of-arrival isoplanatism in the case of daytime high angular resolution imaging for which the promising results of adaptive optics in the stellar field (Primmerman et al. 1991; Fugate et al. 1991) could be applicable. In the first part are reviewed the different concepts and useful theoretical results together with measurement techniques for isoplanatic patch size estimation. A subsequent method for evaluating the angle-of-arrival isoplanatism in the case of solar observations is introduced. An experiment is described and some experimental results obtained on the site of Calern (CERGA-Grasse-France) are presented. Finally, using a modelization proposed by Fried (1977), a vertical localization of the turbulence "optical strength" $C_n^2(h)$ (structure constant of the air-refractive-index fluctuations) is deduced, which leads to the estimation of the isoplanatic patch sizes for adaptive optics and speckle interferometry.

2. Isoplanatism. Theoretical aspects

Atmospheric turbulence causes perturbations on the wavefront coming from a point source which gives at ground level, random fluctuations of the phase and of the intensity. One considers frequently only the phase fluctuations (near-field approximation); one observes the point spread function in the focal plane as an image of speckles,

Send offprint requests to: J. Borgnino

which have spatio-temporal dependence. Speckle formation is due to the random phase differences which create an interferogram in the focal plane. The number of speckles in the image is of the order of $(D/r_0)^2$ where D is the pupil diameter and r_0 is the so-called Fried's parameter which is related to the size of the coherence areas of the wavefront arriving at the entrance of the telescope pupil. The image motion is due to the angle formed by the pupil plane with the wavefront slope all over the pupil; this defines an averaged angle of arrival which may be also considered at each point of the wavefront.

This isoplanatism expresses in a general way, the similarity of the wavefronts arriving on the pupil from two point sources separated by an angle θ on the sky and which have traversed different zones of the turbulent atmosphere. According to the desired application, which can be categorised by the features of interest in the images, a precise analysis of the wavefront deformations can be done which implies the definition of several types of isoplanatism. In the framework of this study, the classification introduced by Fried (1976) has been used, but limited to the case of isoplanatism relevant to angle-of-arrival observations, and also for adaptive optics and speckle interferometry for which the general concepts are reviewed.

The angle-of-arrival isoplanatic patch is the angular field of view on which one can consider that all image points are subjected to the same motion effect which results from the averaging of the angle-of-arrival fluctuations over a pupil of diameter equal to D. It expresses in fact, the angular covariance of these fluctuations observed on two lines of sight separated on the sky by θ. To characterize this isoplanatism, it is convenient to make use of the structure function $D_I(\theta)$ defined as:

$$D_I(\theta)=\langle[\alpha(\theta_1)-\alpha(\theta_1+\theta)]^2\rangle,$$

where $\alpha(\theta_1)$ describes the angle-of-arrival fluctuations averaged over a pupil of diameter D for the wavefront coming from a source in the direction θ_1 and $\langle\ \rangle$ symbolizes a set mean.

An analytic expression for $D_I(\theta)$ has been established by Fried (1976) whose later approximate form (Fried 1977) we use:

$$D_I(\theta)=D^{-1/3}\int_{\text{Path}} C_n^2(h)\ F(h,\theta)\,dh, \tag{1}$$

where h denotes the altitude and

$$F(x)=5.98\left(1+\left(\frac{0.864}{x}\right)^2\right)^{-1} \quad \text{with} \quad x=\frac{\theta h}{D}.$$

The analytic expression has been calculated numerically and compared to the approximate form. A good agreement between the two expressions has been found and for conciseness, the second one will be used hereafter.

According to the definition given by Fried (1977), the isoplanatic patch is:

$$\theta_{AOA}=0.864\frac{D}{h_{AOA}}, \quad \text{where} \quad h_{AOA}=\left[\frac{\int h^2 C_n^2(h)\,dh}{\int C_n^2(h)\,dh}\right]^{1/2}. \tag{2}$$

The speckle interferometry isoplanatism corresponds to the angular field over which one can consider that the speckle interferograms obtained when one observes two point sources separated by θ are the same, according to a given criterion. Its expression can be found by considering the cross-correlation between the corresponding optical transfer functions which can be expressed according to the complex amplitude second-order moment $B_\theta(f)$ (Fried 1979; Roddier et al. 1982):

$$B_\theta(f)=\langle\psi(u,\theta_1)\,\psi(u+f,\theta_1+\theta)\rangle$$

In the case of a fully-developed turbulence (Kolmogorov's law) and for $D\gg r_0$, this moment can be expressed by:

$$B_\theta^2(f)=\exp\left(-6.88\left(\frac{\lambda}{r_0}\right)^{5/3}\frac{\int\left|f+\frac{\theta h}{\lambda}\right|^{5/3}C_n^2(h)\,dh}{\int C_n^2(h)\,dh}\right). \tag{3}$$

The isoplanatic patch for speckle interferometry can be obtained by integrating expression (3):

$$\theta_{SP}=0.36\frac{r_0}{h_{SP}},$$

$$\text{where} \quad h_{SP}=\left[\frac{\int h^2 C_n^2(h)\,dh}{\int C_n^2(h)\,dh}-\left[\frac{\int hC_n^2(h)\,dh}{\int C_n^2(h)\,dh}\right]^2\right]^{1/2}. \tag{4}$$

For adaptive optics, the isoplanatic patch is the angular field on the sky where one can consider that the wavefronts coming from two points sources angularly separated by θ and arriving on the same point in the pupil plane of the instrument are similar according to a given criterion. The expression for isoplanatic patch can also be deduced from the relation (3) by calculating $B_\theta(0)$ (Roddier et al. 1982):

$$\theta_{AO}=0.31\frac{r_0}{h_{AO}}, \quad \text{where} \quad h_{AO}=\left[\frac{\int h^{5/3} C_n^2(h)\,dh}{\int C_n^2(h)\,dh}\right]^{3/5}. \tag{5}$$

One can see that in every case, knowledge of the vertical profile of the optical strength $C_n^2(h)$ permits the estimation of the isoplanatic patch which can be interpreted using a model (Shapiro 1976) in which a single thin layer is localized at an altitude (h_{AOA}, h_{SP}, h_{AO}) defined by a weighting of $C_n^2(h)$ [Expressions (2), (4) and (5)].

Another remark is that when observing with a small aperture telescope, the size of the isoplanatic patch will not differ considerably for one type of isoplanatism to another but will vary notably for large astronomical telescopes.

3. Measurement techniques

Several techniques have been used to estimate the isoplanatic patch. Some of them give direct measurements,

other use an intermediate parameter and a model to describe the terrestrial atmosphere. In the following we give some techniques which permit isoplanatic patch estimations and some typical values obtained by observers.

Various measurements of isoplanatic patch for stellar speckle interferometry and adaptive optics were performed in the visible by Roddier et al. (1982) who derived the parameter using turbulence profiles $C_n^2(h)$ and applying the expressions (4) and (5). The measurements show that for speckle interferometry, the isoplanatic patch is systematically more important (mean value of the order of 3 arcsec) than for adaptive optics (mean value of the order of 2 arcsec). From the cross-correlation function of double star speckle interferograms, Vernin et al. (1991) deduce the degree of isoplanatism (Fried 1982) and derive an estimation of the isoplanatic angle. Using the SCIDAR technique which consists of a statistical analysis of scintillation patterns, permits these observers to obtain turbulence profiles $C_n^2(h)$ and with seeing measurements to compute the isoplanatic patch for speckle interferometry. These two techniques give the same estimate of the isoplanatic patch which is of the order of 3.6 arcsec. Direct measurements of the isoplanatic patch were performed by Walters (1985) who developed a stellar scintillometer from an approximation of Fried's expression (1982) for given light wavelength and telescope diameter. The conception of an isoplanometer which is also a stellar scintillometer is due to Loss & Hogge (1979) and White & Garvey (1985) who have performed continuous measurements of the isoplanatic patch for speckle interferometry. The mean value of the measurements is of the order of 1 arcsec which is smaller than the results of other observers.

For solar observations, there are fewer isoplanatism measurements than for night observations. One can first reference the experiment of Borgnino & Martin (1977) who analysed the spatio-temporal characteristics of the wavefronts arriving on the pupil by observing it through two diaphragms placed on the solar limb image. They observed that some wavefront areas stayed correlated on an angular field which might be extended. Turbulence profile measurements $[C_n^2(h)]$ in daytime conditions allowed to Murphy et al. (1985) to compute from Fried's expression (1979) isoplanatic patch estimates which typically were of the order of 1–2 arcsec. Finally, adaptive optics techniques were used to obtain high angular resolution solar images (Hardy 1981; Acton 1988; Rimmele & Von der Lühe 1988). For these experiments it has been assumed that the maximum value reached by the isoplanatic patch was of the order of 3 or 4 arcsec. A value of the same order was also used in the framework of post-detection reconstruction methods (Von der Lühe 1988).

4. Isoplanatic patch measurement using a photoelectric detector

The point spread function of the atmosphere–telescope system can be obtained by observing an unresolved star or, in the case of solar observations, by considering the brightness discontinuity formed by the solar limb. In a first approximation, the solar limb intensity can be considered, taking into account the resolving power of the instrument and the wavelength at which the observations are performed, as an Heaviside distribution $H(\alpha)$ (Druesne et al. 1983). Indeed, if a one-dimensional detector such as a linear photodiode array is put perpendicularly to the solar image edge (Fig. 1a), one can write, assuming that each photoelement is of negligible width and moreover that its physical properties are not taken into account, the detector spatio-temporal response $F(\alpha, t)$ (Fig. 1b) as:

$$F(\alpha, t) = [H(\alpha) * S(\alpha, \beta, t)]\delta(\beta), \quad (6)$$

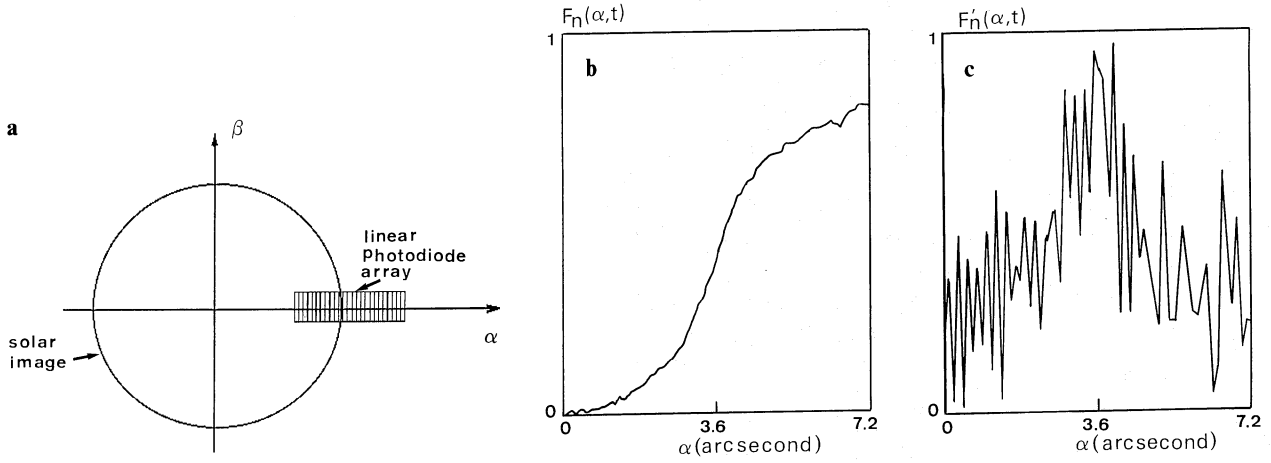

Fig. 1a–c. Estimation of the point spread function of the telescope–atmosphere system obtained at the Nice Observatory using a 38 cm solar telescope: **a** principle of the experiment, α, β = angular directions on the sky; **b** $F_n(\alpha, t)$ = normalized irradiance distribution in the solar limb image [Expression (6)]; **c** $F'_n(\alpha, t)$ = normalized point spread function of the telescope-atmosphere system [Expression (7)]

where $*$ denotes a convolution product, α and β are the components of an angular direction on the sky, $S(\alpha, \beta, t)$ is the point spread function of the system formed by the atmosphere and the telescope and δ the Dirac distribution.

If this expression is derived with respect to α, one obtains the one dimensional point spread function as already presented in Druesne et al. (1983):

$$F'(\alpha, t) = [\delta(\alpha) * S(\alpha, \beta, t)]\delta(\beta) = \delta(\beta) \int S(\alpha, \eta, t)\, d\eta. \quad (7)$$

This expression shows that one should obtain experimentally a one-dimensional projection of the point spread function (Fig. 1c). Thus, the continuous acquisition of the solar image formed on the detector gives the point-spread-function temporal evolution which allows estimation of the parameters qualifying the atmospheric turbulence or more precisely the perturbed wavefronts (r_0, time constants, isoplanatic patch size).

For the angle-of-arrival isoplanatism study, there are two possibilities according to whether one uses a one or a two-dimensional detector.

The angle-of-arrival isoplanatism can be studied using a linear photodiode array, with rectangular elements (the ratio between the two dimensions being for example of the order of 100). In the following, the detector is assumed to have a linear intensity response. Indeed, if the linear photodiode array is placed on the solar image in a direction parallel to the limb (Fig. 2a), each photoelement response will be the solar limb intensity distribution integrated on a few arcseconds. This integration will lead to a solar limb position for each observation field point defined by each photoelement (Fig. 2b). The continuous image acquisition allows to observe and record the solar limb fluctuations (image motion) (Fig. 2c) for which a spatio-angular correlation leads to an estimation of the angle-of-arrival isoplanatic patch size.

The advantage of the method is the simplicity of the application for estimating in real time the parameter of interest. The main difficulties are related to the spatial calibration of the fluctuations and to the dynamics which is imposed by the continuum of the mean position, more or less important, of the solar image on the detector.

The use of a two-dimensional detector as a CCD camera gives access to more information and makes it possible the estimation of all the parameters qualifying the terrestrial atmosphere and consequently the astronomical images. Indeed, as for the preceding case, the CCD camera is put on the edge of the solar image (Fig. 3). Each line of the camera gives a solar limb profile which allows to deduce a projection of the point spread function of the whole system, telescope and atmosphere, as seen in the previous section [Expression (7)]. The image acquisition gives then, a spatio-temporal evolution of the point spread function for an angular field on the sky. From this evolution, one can deduce the angle-of-arrival isoplanatic patch size from the angular correlation of the fluctuations shown by the position of the point spread function projection defined as the position of the photocenter. A study of the correlation between the point spread functions obtained from the different line signals (perpendicular to the solar limb) of the CCD camera, leads to perform a speckle interferometry type analysis if a spectral filtering is done on the solar image.

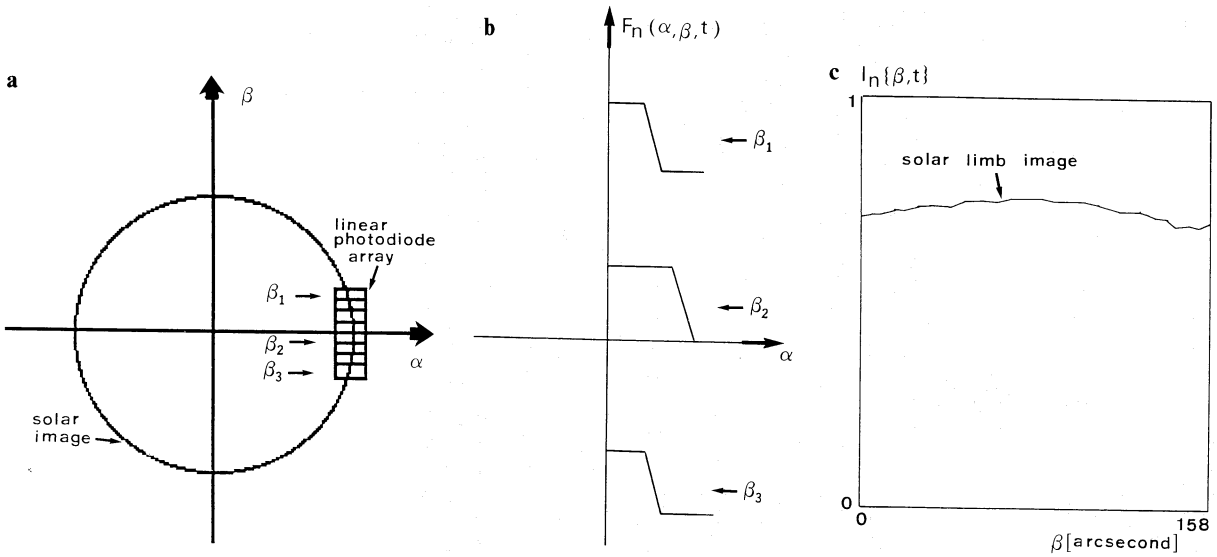

Fig. 2a–c. Estimation of the angle-of-arrival isoplanatic patch size using a linear photodiode array with the same experimental device as for the result presented in Fig. 1: **a** principle of the experiment; **b** schematic examples of the solar limb profile; **c** normalized solar limb intensity with the continuum before analogic–numerical conversion. One will note the small magnitude of the fluctuations averaged according to the angular component α, on a range of the order of 100 arcsec

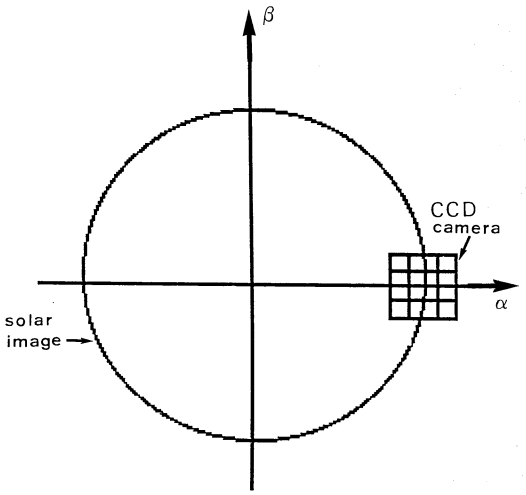

Fig. 3. Estimation of the angle-of-arrival isoplanatic patch size (and eventually, of the spatial coherence of the perturbed wavefronts as expressed using Fried's parameter r_0, of the time constants ...). The principle of the experiment is given if the detector in use is a CCD camera

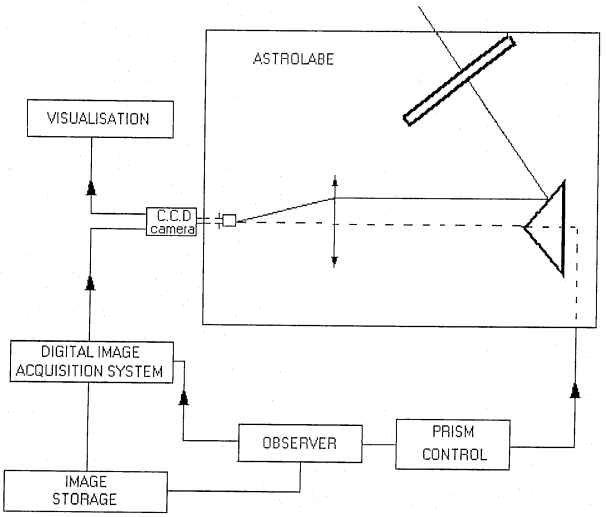

Fig. 4. The data acquisition device. The instrument is widely described in the paper of Laclare & Merlin (1991)

5. Observations and results

The measurements have been performed making use of the experimental principle detailed in the previous section but with the difference that the observed solar limb image is moving in the focal plane during the observation time. The instrument is a Danjon astrolabe which does not compensate the earth diurnal motion.

5.1 Observations

The observations have been made using the solar astrolabe of the Calern Observatory (Observatoire de la Côte d'Azur) which is currently used for solar diameter measurements (Laclare & Merlin 1991). For the study of atmospheric turbulence, the experiment has been modified. These modifications consist for the main part, in the two following points:

— the analogic detection system of the solar limb inflexion point given by a CCD camera which provides 512×512 pxl, has been replaced by a digital image acquisition system.

— the astrolabe is an instrument which gives in its focal plane two images of the same object (a direct and a reflected image). For the solar diameter measurements, the two images are used and formed alternatively on the CCD camera by a mechanical obturator. For this experiment, the obturator is removed and only the direct image formed by the upper part of the objective which has an elliptic form (the major axis is 8 cm and the minor 5 cm) is used. Because of the limited memory of the system and to process a greater number of images, a window of 128×256 pxl has been placed on the solar image.

Figure 4 shows the data acquisition device.

An acquisition of the solar limb image is done every 20 ms which is the standard integration time of the camera. The fluctuations of the images are attributed to the motion effect, the result of the angle-of-arrival fluctuations observed at each wavefront point, averaged on the astrolabe pupil during the integration time of the camera. In the case of an unresolved solar limb from which one can define the point spread function position as the photocenter position, each point of the image edge is affected only by the motion effect. The displacement fluctuations obtained by observing the temporal evolution of a part of the solar image will then give an estimation of the angle-of-arrival structure function which allows one to deduce the value of the associated isoplanatic patch.

5.2. Results

The experimental results presented here come from observations performed in June 1990 at the Calern Observatory. In Fig. 5a one can see two estimations of the angle-of-arrival structure function $D_l(\theta)$ [Expression (1)] obtained from the computational data of two different observation days. In this figure no correction has been done but one must take into account the noise effects on the structure or autocorrelation function analysis. So let's consider hereafter the noise effects. One supposes that a white noise is superposed on the fluctuation signal measurements which is translated on the autocorrelation function (or on the structure function) by a peak located at the origin or on the power spectrum by a uniform energy distribution over all frequencies as clearly observed after the telescope frequency cut-off (Aime et al. 1979). Consequently, to estimate the noise level, one considers the power spectrum and also the behaviour of the structure function of the

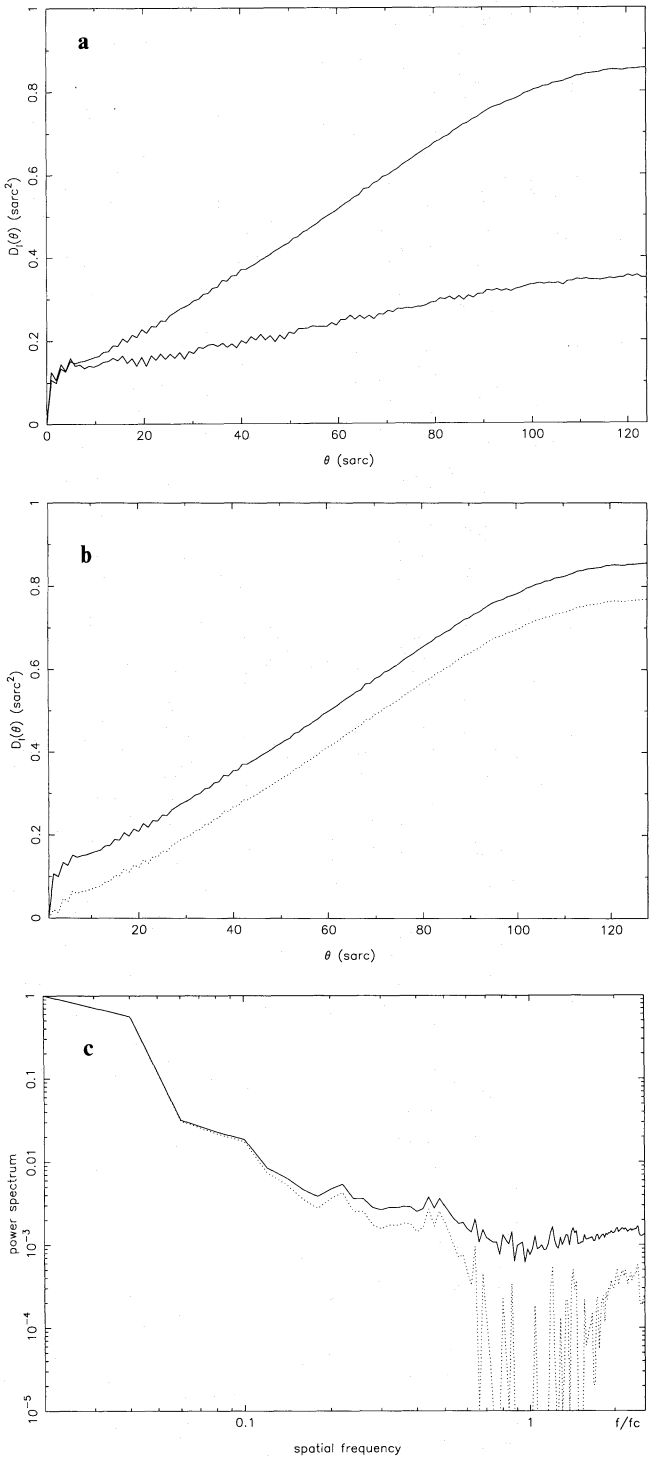

Fig. 5a–c. Experimental estimations of the angle-of-arrival structure function obtained observing the solar limb motion (without noise correction **a**). Effect of the correction of the photon noise on a typical estimation of the angle-of-arrival structure function **b** and on the corresponding power spectrum **c**

angle-of-arrival fluctuations for small values of θ as done by Fried (1977). Indeed, to define the isoplanatic patch Fried has considered the intersection between a parabolic fit of the structure function $D_I(\theta)$ for small values of θ and the straight line giving the saturation of this function for large values of θ. Fried's definition leads to the relation (2) in Sect. 2 which gives the angle-of-arrival isoplanatic patch size as a function of the pupil diameter D and of the altitude h_{AOA} of an impulse layer equivalent to the whole turbulent atmosphere (an experimental illustration is given in Fig. 6). To have a noise level estimate, one fits the structure function by a parabolic law where the first point is not included and deduces its value from the fit. One can see in Fig. 5b the effect of the noise correction on a typical structure function and in Fig. 5c the corresponding effect on the power spectrum. In the last case, one can note the effect of the noise level reduction on the high spatial frequencies while the low frequencies are not notably affected as identically observed by Aime et al. (1979). However, from the data coming from all the observations, one can note that there is not one single way to fit a parabolic law for small values of θ but that this can be performed on two distinct angular ranges (Fig. 7). According to Fried's definition and for two series of observations are shown, in Table 1, the results deduced from parabolic fits in the two typical variation ranges of the structure function. The first range corresponds to the variation of the structure function at the origin which expresses the fast angle-of-arrival fluctuations averaged on the instrument pupil and the second range corresponds to the slowest variation of this structure function. Determination of isoplanatic patch sizes from these two variation ranges seems identical to that performed by other observers who deduced two different time constants from the measurement of the temporal autocorrelation function obtained by analysing during the time, the brightness intensity of the solar granulation (Aime et al. 1981). For night observations, the same results

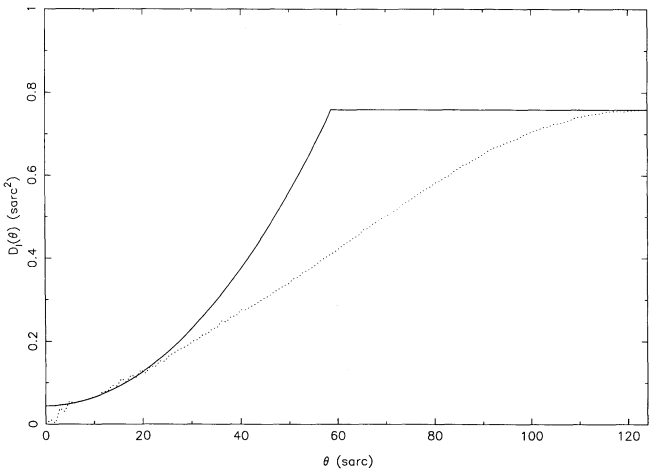

Fig. 6. Estimation of the isoplanatic patch size using a parabolic fit (continuous line) near the origin of the experimental structure function (dotted line) obtained from the observation of the angle-of-arrival fluctuations. The horizontal straight-line gives an approximated value of the saturation which occurs at large values of θ

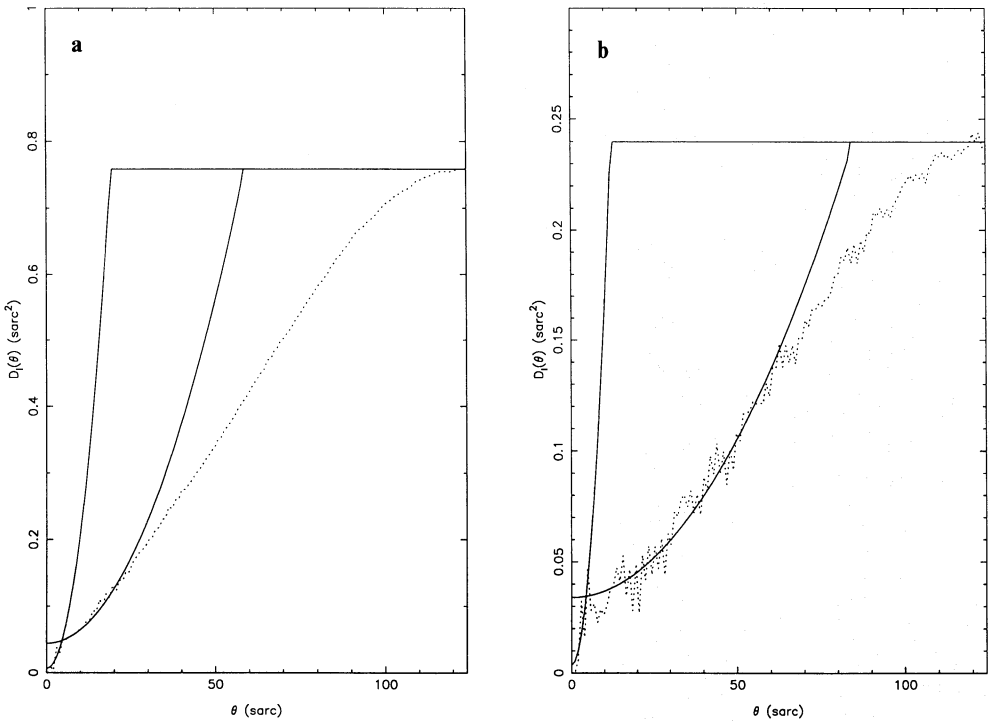

Fig. 7a and b. Possible fits (continuous lines) on two examples of the experimental angle-of-arrival structure function (dotted line) in order to estimate the isoplanatic patch size: **a** date = 21/06/90, $\theta_{AOA1} = 19.3''$, $h_{AOA1,} = 642$ m, $\theta_{AOA2} = 58.8''$, $h_{AOA2} = 210$ m; **b** date = 25/06/90, $\theta_{AOA1} = 12.1''$, $h_{AOA1} = 1024$ m, $\theta_{AOA2} = 84.9''$, $h_{AOA2} = 146$ m

Table 1. Isoplanatic patch size: experimental results From this two-layer model are computed the isoplanatic patch sizes and the corresponding altitudes h_{AO}, h_{sp}, h_{AOA} (Expressions (5), (4) and (2)) for adaptive optics, speckle interferometry and for the angle-of-arrival fluctuations

Date	21/06/90	21/06/90	21/06/90	25/06/90	25/06/90	25/06/90
r_0 (cm)	11.2	6.7	7	12.4	13.8	10.2
H_{AOA1} (m)	1046	642	1365	1092	1024	931
Isoplanatic patch Range 1 (arcsec)	11.83	19.28	9.07	11.33	12.09	13.29
H_{AOA2} (m)	164	210	154	146	146	145
isoplanatic patch Range 2 (arcsec)	75.70	58.81	80.44	84.58	84.85	85.62
isoplanatism adaptive optics (arcsec)	4.9	3.8	2.2	5.8	5.8	5.7
isoplanatism speckle interferometry (arcsec)	4.4	3.3	2.2	5.1	5.3	4.9
isoplanatism angle-of-arrival (arcsec)	5.4	6.7	4.1	5.7	5.2	6.7
h_{AO} (m)	1474	1139	2043	1372	1524	1140
h_{SP} (m)	1889	1530	2421	1782	1941	1531
h_{AOA} (m)	1984	1592	2604	1866	2041	1593

r_0 = Fried's parameter
H_{AOA1}, H_{AOA2} = altitudes of the two impulse turbulent layers corresponding to the isoplanatic patch sizes (Ranges 1 and 2) which can be deduced from the experimental angle-of-arrival spatio-angular structure function.

have been obtained (Aime et al. 1986; Scaddan & Walker 1978) and an interpretation has been proposed in the case of stellar speckle patterns introducing a new model based on the image motion (Aime et al. 1986).

6. Discussion

The results presented above show that the experimental structure function $D_I(\theta)$ has two variation ranges on which can be defined two isoplanatic patch sizes. The shape of $D_I(\theta)$ is related to the vertical atmospheric turbulence profile (see Sect. 2); one can then assume, in a first approximation, that each variation corresponds independently to a thin turbulent layer localized at an altitude h_{AOA} which can be estimated by (Fried 1977):

$$h_{AOA} = \frac{D}{\theta_{AOA}},$$

where D is the diameter of the instrument pupil.

One can then, with this assumption, locate the layers responsible for the two variation ranges presented by the structure function $D_I(\theta)$. The fast variation is due to a layer localized at the higher altitude whereas the slower variation is due to a layer at a lower altitude. In Table 1, one can also found, for each isoplanatic patch, the altitude of the associated turbulence layer. In Figs. 8b and 9b are presented the vertical C_n^2-profiles for both Hunfnagel model (daytime conditions) and the restored profile which corresponds to the experimental structure functions. For each layer, the turbulence strength is chosen to fit the angle-of-arrival structure function, computed from the relation (1) (see Sect. 2), to the experimental data (Figs. 8a and 9a). One can note that for the two cases, one can access to a vertical C_n^2-profile which explains correctly the observations and defines, as already said above, the magnitude of the different isoplanatic patch sizes. Thus, with a simple model of two thin layers and the relations given in Sect. 2, one can deduce an estimate of the isoplanatic patch for adaptive optics, speckle interferometry and angle-of-arrival fluctuations using only an angle-of-arrival statistical analysis. It must be noted that one can also deduce the angle-of-arrival isoplanatic patch from the relation (3) which is equivalent to a parabolic fit at the origin of $D_I(\theta)$. From this relation, one obtains values more or less different than those derived from the fit on the experimental data done using a least-mean-square adjustment on a chosen angular field which can be overestimated compared with Fried's hypothesis in the approximate form. For each observation series, performed at a wavelength equal to 500 nm, an estimate of a vertical C_n^2-profile has been done which allows to compute estimates of Fried's parameter r_0, as well as the isoplanatic patch for adaptive optics θ_{AO}, for speckle interferometry θ_{SP}, for angle-of-arrival fluctuations θ_{AOA} and the scale heights for the single thin layer model (Table 1). It is advisable to note that for speckle interferometry determination, the expression implies that D is great compared to r_0 which is not true for our observations. The value has been computed to give an estimate of this parameter which appears to be comparable with the other values. One can see that for all

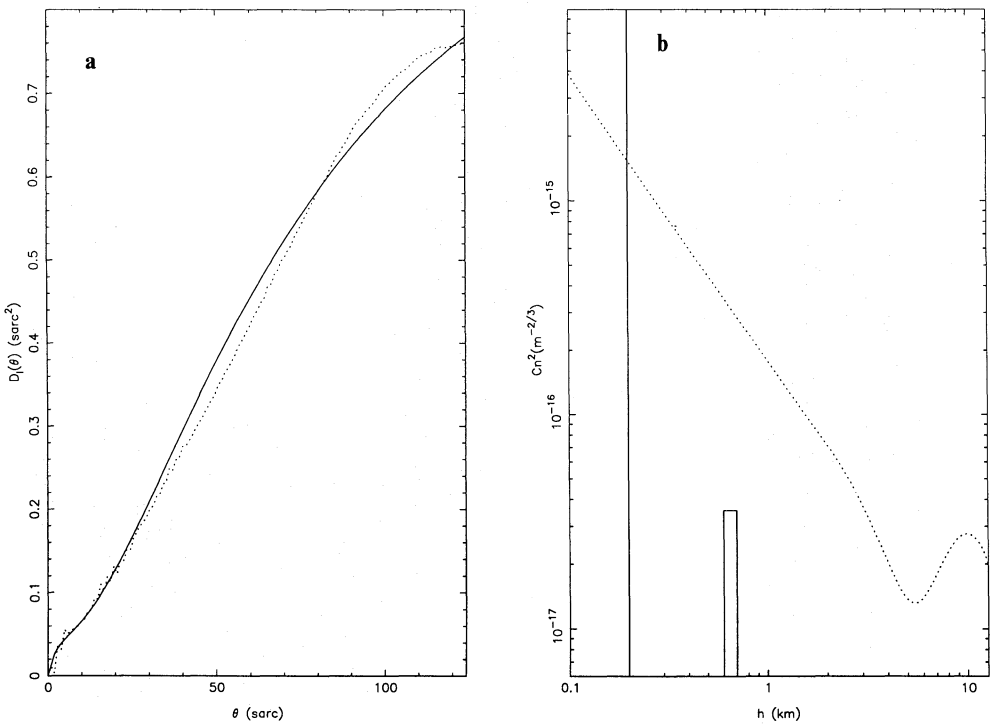

Fig. 8a and b. Interpretation of the experimental angle-of-arrival structure function using a two-layer model to describe the atmospheric turbulence – Example (a) of Fig. 7: **a** (… …) experimental result; (——) function deduced from relation (1) when the turbulence is given by a two-layer distribution (see b); **b** (——) model of turbulence; (… …) Hufnagel mean model-daytime conditions

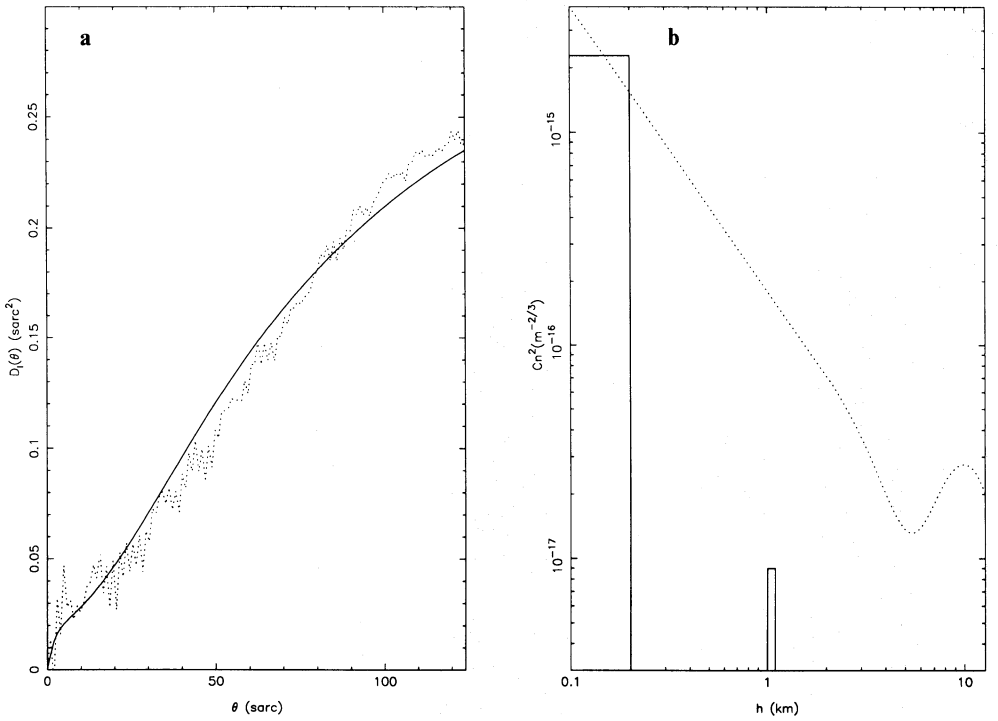

Fig. 9a and b. Interpretation of the experimental angle-of-arrival structure function using a two-layer model to describe the atmospheric turbulence – Example (b) of Fig. 7: **a** (... ...) experimental result; (——) function deduced from relation (1) when the turbulence is given by a two-layer distribution (see b); **b** (——) model of turbulence; (... ...) Hufnagel mean model-daytime conditions

cases, the estimate is of the same order but more larger than those reported by other observers (see Sect. 3). Finally, one can note, analyzing the estimated vertical C_n^2-profiles, that the atmospheric turbulence relevant to high spatial resolution solar imaging is localized in the first hundred meters.

7. Conclusion

The principle of a method which allows the measurement of the angle-of-arrival isoplanatic patch for day-time observations has been presented. The results deduced from observations performed using the solar astrolabe of Calern Observatory (CERGA-France), show that the experimental structure function $D_I(\theta)$ has two variation ranges on which an isoplanatic patch size can be estimated. The interpretation of these two variation ranges can easily be done by the use of a simple model of two thin layers; the associated vertical turbulence C_n^2-profile has been obtained by fitting the experimental data using a procedure proposed by Fried (1977). This estimated vertical C_n^2-profile which, in all cases, imposes the magnitude of the isoplanatic patch, has allowed to compute an estimate of the isoplanatic patch for the angle-of-arrival fluctuations, but also in the framework of speckle interferometry and adaptive optics. For all cases, the estimation is globally of the same order but notably larger than the values reported by other observers. To conclude, we emphasize that anisoplanatism may appear at different scales related to a small number of impulse turbulent layers which forms an equivalent vertical profile. This is important when observing extended astronomical objects at high spatial resolution.

References

Aime C., Kadiri S., Ricort G., Roddier C., Vernin J., 1979, Optica Acta 26, 575–581
Aime C., Kadiri S., Martin F., Ricort G., 1981, Opt. Commun. 39, 287–292
Aime C., Borgnino J., Kadiri S., Martin F., Petrov R., Ricort G., 1986, J. Opt. Soc. Am. 3, 1001–1009
Acton D.S., 1988, in: Von der Lühe O. (ed.) Proc. 10th Sacramento Peak Summer Workshop, High Spatial Resolution Solar Observations, 22–26 August, Sunspot, New Mexico, p. 71
Borgnino J., Martin F., 1977, J. Opt. (Paris) 8, 319–326
Chassat F., 1989, J. Opt. (Paris) 20, 13–23
Druesne P., Borgnino J., Aime C., Petrov R., Kadiri S., 1983, J. Opt. (Paris) 14, 11–17
Foy R., Labeyrie A., 1985, A&A 152, L29–L31
Fried D.L., 1976, SPIE 75, 20–29
Fried D.L., 1977, in: High Angular Resolution Stellar Interferometry, Colloquium no 50 (U.A.I.), 4.1–4.44
Fried D.L., 1979, Opt. Acta 26, 597–613
Fried D.L., 1982, J. Opt. Soc. Am. 72, 52–61
Fugate R.Q., Fried D.L., Ameer G.A., Boeke B.R., Browne S.L., Roberts P.H., Ruane R.E., Tyler G.A., Wopat L.M., 1991, Nat 353, 141–143
Hardy J.W., 1981, in: Dunn R.B. (ed.) Solar Instrumentation: What's Next? p. 421
Laclare F., Merlin G., 1991, C. R. Acad. Sci. (Paris) 313, 323–330
Loss G.C., Hogge C.B., 1979, Appl. Opt. 18, 2654–2661
Murphy E.A., Dewan E.M., Sheldon S.M., 1985, SPIE 551, 156–162

Primmerman C.A., Murphy D.V., Page D.A., Zollars B.G., Barclay H.T., 1991, Nat 353, 141–143
Rimmele T., Von der Lühe O., 1988,in: Von der Lühe O. (ed.) Proc. 10th Sacramento Peak Summer Workshop, High Spatial Resolution Solar Observations, 22–26 August, Sunspot, New Mexico. p. 90
Roddier F., Gilli J.M., Vernin J., 1982, J. Opt. (Paris) 13, 63–70
Scaddan R.J., Walker J.G., 1978, Appl. Opt. 17, 3779–3784
Sechaud M., Fontanella J.C., Rousset G., Primot J., Chassat F., 1990, SPIE 1312, 58–71
Shapiro J.H., 1976, J. Opt. Soc. Am. 66, 469–477
Vernin J., Weigelt G., Caccia J.L., Müller M., 1991, A&A 243, 553–558
Von der Lühe O., 1988, in: Von der Lühe O. (ed.) Proc. 10th Sacramento Peak Summer Workshop, High Spatial Resolution Solar Observations, 22–26 August, Sunspot, New Mexico. p. 147
Walters L., 1985, SPIE 551, 38–41
Welsh B.M., Gardner C.S., 1991, J. Opt. Soc. Am. 8, 69–80
White K.O., Garvey D.M., 1985, SPIE 551, 163–169